Nonlinear localized modes in two-dimensional electrical lattices

L.Q. English,[1] F. Palmero,[2] J.F. Stormes,[1] J. Cuevas,[2] R. Carretero-González,[3] and P.G. Kevrekidis[4]

[1]*Department of Physics and Astronomy, Dickinson College, Carlisle, Pennsylvania, 17013 USA*
[2]*Nonlinear Physics Group. Escuela Técnica Superior de Ingeniería Informática. Departamento de Física Aplicada I. Universidad de Sevilla. Avda. Reina Mercedes, s/n. 41012-Sevilla (Spain)*
[3]*Nonlinear Dynamical Systems Group, Department of Mathematics and Statistics, and Computational Science Research Center, San Diego State University, San Diego CA, 92182-7720, USA*
[4]*Department of Mathematics and Statistics, University of Massachusetts, Amherst, Massachusetts 01003-4515, USA*

We report the observation of spontaneous localization of energy in two spatial dimensions in the context of nonlinear electrical lattices. Both *stationary and traveling* self-localized modes were generated experimentally and theoretically in a family of two-dimensional *square*, as well as *honeycomb* lattices composed of 6×6 elements. Specifically, we find regions in driver voltage and frequency where stationary discrete breathers, also known as intrinsic localized modes (ILM), exist and are stable due to the interplay of damping and spatially homogeneous driving. By introducing additional capacitors into the unit cell, these lattices can *controllably* induce traveling discrete breathers. When more than one such ILMs are experimentally generated in the lattice, the interplay of nonlinearity, discreteness and wave interactions generate a complex dynamics wherein the ILMs attempt to maintain a minimum distance between one another. Numerical simulations show good agreement with experimental results, and confirm that these phenomena qualitatively carry over to larger lattice sizes.

Introduction. It has long been known that solitons emerge as classes of solutions to many nonlinear (lattice and partial) differential equations described chiefly by one spatial dimension; prominent examples are the KdV equation, the sine-Gordon or the nonlinear Schrödinger equations. In two dimensions, quasi one-dimensional localization patterns can often still occur [1], but robust two-dimensional (2D) localization in continuous media is rather atypical (see Ref. [2] and references therein). However, it is well-known that discreteness of the underlying medium can help to stabilize such localized solutions even in higher dimensions [3, 4]. Alternatively, one can externally enforce or introduce a periodicity in the form of a regular modulation in some property of the continuous (e.g. in optical photorefractive or atomic Bose-Einstein condensate) media [5, 6], thus again breaking continuous translational symmetry.

Here we show that two-dimensional discrete breathers, also known as intrinsic localized modes (ILMs), *experimentally* exist and are stable in the context of two-dimensional, damped-driven electrical lattices. We characterize these breather and multi-breather states in parameter space, and we compare to numerical simulations and stability analysis. Finally, we focus particularly on versions of these lattices that support moving breathers. Discrete breathers have been considered in a variety of other settings experimentally including (but not limited to) micromechanical cantilever arrays [7], Josephson-junction ladders (JJLs) [8], granular crystals of beads interacting through Hertzian contacts [9], layered antiferromagnetic crystals [10], halide-bridged transition metal complexes [11], and dynamical models of the DNA double strand [12]. Yet, in most of these examples, the coherent structures are effectively one-dimensional. Even when higher dimensional (as is e.g. possible in optical waveguide arrays or photorefractive crystals [5]), the states are typically stationary. Hence, the experimental ability to systematically generate discrete breathers in two-dimensional electrical lattices and, perhaps especially, to control their mobility launches a new dimension in the modeling, and the theoretical and experimental understanding of such states. This may be of broader interest in other areas as well, such as JJLs (see e.g. the theoretical proposal of Ref. [13]) and two-dimensional granular crystals (see e.g. the recent experimental realization of Ref. [14]). Another attractive feature of our lattices is their potential square or honeycomb geometry, especially since the latter has been a point of intense investigation at both the linear and the nonlinear level. This is due to its conical diffraction and Dirac (diabolical) points examined intensely in both the physical [15, 16] and mathematical [17] communities, as well as due to potential connections with graphene nano-ribbons; see e.g. [18, 19] and references therein.

Experimental and theoretical setup. The experimental system under investigation is a class of two-dimensional electrical lattices of either honeycomb or square geometry, as shown in Fig 1. These electrical lattices can be considered as a set of single cells representing nonlinear LC oscillators, each composed of a varactor diode (NTE 618) with a nonlinear capacitance $C(V)$ and an inductor $L_2 = 330 \ \mu$H. These single cells are then coupled at point V by inductors $L_1 = 680 \ \mu$H and are driven by a single sinusoidal voltage source $V(t)$ via a resistor $R = 10 \ k\Omega$, with amplitude V_d and frequency f. We study two different unit cell versions, with the only dif-
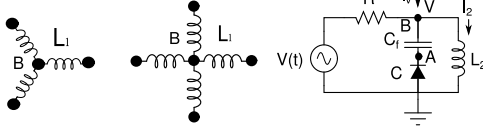
FIG. 1: Left: Schematic circuit diagrams of the basic geometry of the two electrical transmission lines (honeycomb and square), where black points represent single elements (right), with or without the block capacitor C_f.
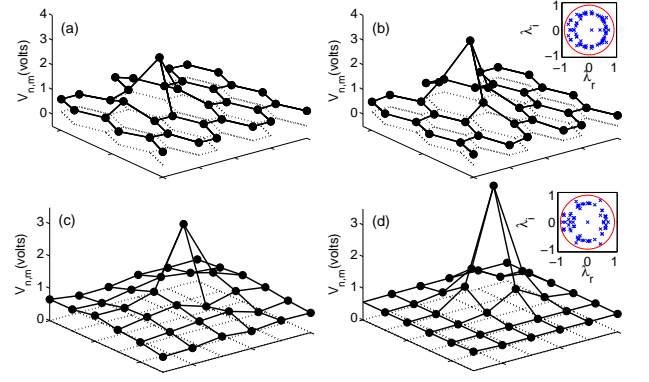

FIG. 2: (color online) Comparison between the experimental ((a) and (c)) and numerical ((b) and (d)) profiles of stationary one peak breathers in a honeycomb lattice, (a) and (b), and a square lattice, (c) and (d). The insets show the Floquet numerical linearization spectrum, confirming (since all multipliers are inside the unit circle) the stability of solutions. The driver has amplitude and frequency $V_d = 1.5$ V and $f = 283$ kHz in the honeycomb lattice case, and $V_d = 2$ V and $f = 290$ kHz (experimental) and $f = 301$ kHz (numerical) in the square lattice case.

ference being the presence of a block capacitor between the diode and the coupling inductor in one of them, as explained in Ref. [20]. The effect of the block capacitor is to make ILMs mobile; here we study two different values of block capacitances, $C_f = 1$ μF and $C_f = 15$ nF. The experimental lattices were comprised of 36 elements with periodic boundary conditions, and node voltages $V_{n,m}$ were measured at a rate of 2.5 MHz using a multichannel analog-to-digital converter. In the linear limit of small-amplitude plane-waves, we have obtained the dispersion relation, which yields as the lowest frequency (uniform mode) $f_{\min} \cong 312$ kHz, and the highest frequency $f_{\max} \cong 689$ kHz in the square geometry configuration, and $f_{\max} \cong 617$ kHz in the honeycomb lattice. Notice that this highest-frequency mode in the linear spectrum is now above the second-harmonic of the uniform mode in square geometry lattice, and below it, but very close, in the honeycomb configuration.

Using basic circuit theory, in the block capacitor case, the dynamics of the lattice can be described by the equations [21],

$$
\begin{aligned}
\frac{di_{n,m}}{d\tau} &= \frac{L_2}{L_1}\left(\sum_{j,k} v_{j,k}^B - q\, v_{n,m}^B\right) - v_{n,m}^B, \\
\frac{dv_{n,m}^A}{d\tau} &= \frac{1}{c(v_{n,m}^A)}\Bigg[i_{n,m} - i^D(v_{n,m}^A) - \frac{v_{n,m}^B}{C_0\omega_0 R_l} + \\
&\quad \frac{\cos(\Omega\tau)}{C_0\omega_0 R} - \frac{v_{n,m}^A}{C_0\omega_0 R}\Bigg], \\
\frac{dv_{n,m}^B}{d\tau} &= \frac{dv_{n,m}^A}{d\tau} + \frac{C_0}{C_f}\left[i_{n,m} - \frac{v_{n,m}^B}{C_0\omega_0 R_l}\right],
\end{aligned}
\tag{1}
$$

where the sum is taken over first, q, neighbors, $q = 4$ in square lattice case, and $q = 3$ in honeycomb one. Also, the following dimensionless variables were used: $\tau = \omega_0 t$; $i_{n,m} = (I_v - I_2)/(\omega_0 C_0 V_d)$, where I_v is the full current through the unit cell, and I_2 the current through the inductor L_2, both corresponding to cell (n,m); $v = V/V_d$, used with superscripts A and B; $V_{n,m}^B$ is the measured voltage at node (n,m); $V_{n,m}^A$ is the voltage at an intermediate point between the varactor and the block capacitor; $\Omega = 2\pi f/\omega_0$, $\omega_0 = 1/\sqrt{L_2 C_0}$; $i_D = I_D/(\omega_0 C_0 V_d)$,

where I_D is the current through the varactor diode; $c = C(V)/C_0$, where $C_0 = C(0)$, and $C(V)$ is the nonlinear capacitance of the diode. Also, a phenomenological dissipation resistor, R_l, was included in the model to better approximate the experimental dynamics, and its value has been determined by matching the numerical and experimental nonlinear resonance curves corresponding to a single element [21]. A simplified set of equations corresponding to the non–block capacitor case can be obtained by considering the limit $C_f \to \infty$. In all cases, the ratio L_2/L_1 characterizes the strength of the "effective" discreteness of the system.

Results on standing/traveling discrete breathers in square/honeycomb 2D lattices. To generate discrete breathers, we have employed the well-known modulational instability of the driven uniform mode [3]. In the case without block-capacitors, we obtain stationary and stable one-peak breathers, as shown in Fig. 2. These localized modes are *robust*, persisting as long as the driver remains on.

Numerics are generally found to be in good agreement with experimental results. Yet, it can be seen in Fig. 2 that the amplitude of the one-peak breather is slightly higher in the numerics than in the experimental data. We attribute this slight mismatch to energy dissipation in the coupling inductors; these are stronger in the square lattice setting than in the honeycomb geometry, and they are not taken into account in our simplified model of Eq. (1). When this dissipation is included in our model, by means of some phenomenological small resistances in series with inductors L_1, this further improves the agree-
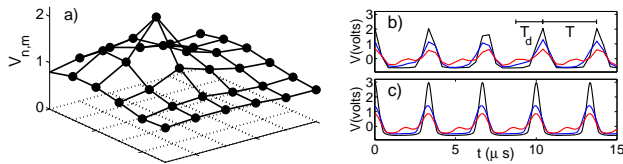
FIG. 3: (color online) Subharmonic breather corresponding to a square lattice, $V_d = 6.4$ V and $f = 600$ kHz. (a) Experimental spatial profile, and (b) experimental and (c) numerical temporal oscillations of three different nodes: the ILM center (black), the first neighbor (blue), and the node furthest away from the ILM center (red). Note that the oscillations of the node furthest away from the ILM center display local maxima corresponding to the natural period T of the ILM at twice the driving period $T_d = 1/f$.

ment for the ILM amplitude. For even higher amplitudes in the experiment, multi-peak breathers have been observed, which can also be captured by the model.
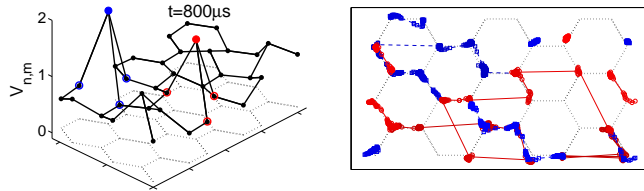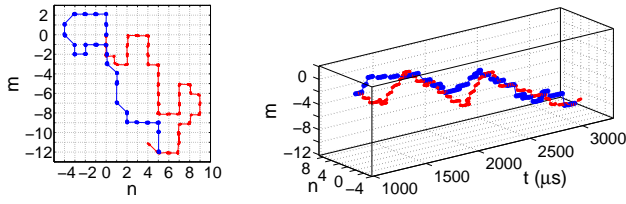
As in the one-dimensional line [22], we again observe subharmonic breathers (experimentally and theoretically) in two dimensions. In Fig. 3, the peak of the breather oscillates with a frequency $f_{\text{ILM}} = f/2$. Notably, in two dimensions it is generally more difficult to stabilize breathers via subharmonic driving —the driving conditions have to fall into a fairly limited region of parameter-space. Further illustrating the fragility of subharmonic breathers in two dimensions, we note that the introduction of block capacitor destroys subharmonic breathers —a qualitative difference with the one-dimensional lattice for which mobile subharmonic breathers were reported. The fact that the frequency of the subharmonic driver, namely twice the ILM response frequency, is now positioned within, or very close to, the linear dispersion band of the 2D lattice may explain this fragility. Our numerical simulations indicate (results not shown here) that in larger lattices, multi-peak subharmonic breathers exist, and such subharmonic breathers appear to be more robust in the absence of block capacitors.

When a block capacitor of 1 μF is placed in series with the diode in the honeycomb and square lattice, the static breathers become mobile, as was the case for the one-dimensional chain [20]. Nevertheless, and contrary to the simpler situation in one dimension, where a clear direction of movement arises, the motion through the lattice appears to be more complex, as shown in Fig. 4. In general, numerical simulations obtained solving Eq. (1) show fairly good agreement with experiments and yield information about the intrinsic nature of this complex motion, where a strong sensitivity to small inhomogeneities is seen. The transition from one node to the next is such that where after a number of periods a noticeable asymmetry develops in the ILM profile; this leads to two neighboring nodes attaining equal amplitude, and

finally the ILM becoming centered (initially between two sites and then) on the next node. This sequence is now also observed in two dimensions. Notice that the mobility problem has been argued to be quite important in other non-square lattices, such as the hexagonal one where breather mobility was proposed as responsible for the presence of dark lines in natural crystals of muscovite mica [23], and reconstructive transformations in layered silicates [24]. In our square electrical lattice, we generally observe (cf. Fig. 4) a directed motion which is interrupted by (longer) intervals of localization as the wave struggles to overcome the well-known Peierls-Nabarro (PN) barrier [3]. Note that given the small size of the lattice, in addition to the role of inhomogeneities, small amplitude residual excitations ("phonons") are also important in directing the breather motion. It is also worth mentioning that, although the movement along the square lattice usually happens along the edges of the lattice, some transitions are also observed to happen, both in the experiment and the numerics, along the diagonals that have a slightly higher PN barrier. Despite the complex nature of the motion of the breathers, the organizing principle obeyed in both one and two dimensions is that the ILM never hops back to the node it occupied prior to its current location due to some residual capacitor-charge impurity associated with that node. In one dimension, this principle necessarily gives rise to orderly, uni-directional motion. In two-dimensional hexagonal lattices there are still two choices available to the ILM, and in a square lattice there are three. Thus, the motion does not have to be uni-directional. It would be interesting to statistically measure the "diffusion" associated with the apparent irregular trajectories displayed by the moving breathers. Although the system is deterministic, due to small defects and residual excitations, the breathers seem to follow a biased erratic motion with the constraint of not going back in the direction they came from. Comparing the scaling of the diffusion associated with this peculiar behavior with the classical Brownian motion and biased random walk variants thereof would be an interesting avenue for future exploration.

In general, multi-peak breathers, or collections of breathers, also become mobile in the lattices with block capacitors. In all of our experimental results, the relevant motion is complex yet the relative distance between peaks remains fairly constant and does not fall below a minimum value (two edges away) (cf. Fig. 5). This observation suggests that two ILMs tend to repel each other upon close proximity. We also note, as in the square lattice, that although most transitions during motion happen through the lattice edges, there are some transitions that happen along the long diagonal of the honeycomb cell (cf. Fig. 5). We note that we did not observe transitions along the short diagonals of the honeycomb cell.

A different scenario takes place when a smaller block capacitance, $C_f = 15$ nF, is chosen. In that case,

FIG. 4: (color online) Trajectory of a one peak moving breather on a square lattice for $V_d = 2$ V, $f = 300$ kHz and $C_f = 1$ μF. Depicted are the positions of the center of mass of the breather in the (n, m) plane (left) and (n, m, t) space (right). The small (red) dots depict the experimental results and the large (blue) dots depict the corresponding numerical simulations. The trajectories have been unwrapped from the periodic lattice. Solid lines have been added for guidance.

FIG. 5: (color online) Left: Experimental two peak moving breather profile on a honeycomb lattice with periodic boundary conditions for $V_d = 2.5$ V, $f = 330$ kHz, and $C_f = 1$ μF. Right: Trajectory of the corresponding centers of mass of the two interacting breathers (circles [red] and squares [blue]). Solid lines have been added for guidance.

breathers become mobile but quickly collapse into a collective pattern resembling a planar (one-dimensional) wavefront, which rapidly transports energy coherently through the system, as shown in Fig. 6. It is intriguing that a spatially homogeneous driver can sustain such nonlinear collective patterns characterized by energy transport. We should point out that the types of coherent patterns experimentally observable in the honeycomb lattice are apparently more complex than in the square lattice where only true planar wavefronts are seen. For the honeycomb lattice the equivalent planar waves, because of the geometry of the lattice, look more complex, and can be found at particular driving frequencies and amplitudes (results not shown here). Numerical simulations performed on larger square lattices (results not shown here) suggest that one-dimensional wavefront profiles are not robust —presumably due to transverse instabilities— and break down into patterns consisting of several ILMs, each one extending over a number of sites. A more detailed account of the phenomenology in larger lattices is currently under investigation and will be reported in a future publication.

Conclusions & future challenges. In summary, we have generated two-dimensional discrete breathers in the setting of damped-driven electrical lattices. To our knowl-
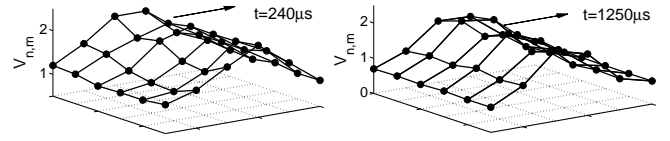

FIG. 6: Experimental (left) and numerical (right) moving front profile for a 6×6 square lattice. $V_d = 2$ V, $f = 300$ kHz and $C_f = 15$ nF.

edge, this is the first time that breathers have been experimentally stabilized in higher-dimensional discrete lattices by direct (and subharmonic) driving, with motion systematically induced to them and that these features have been examined not only in square but importantly also in honeycomb lattices.

We have characterized the statics, stability and mobility of these modes of self-localized energy, centered over a particular node of the lattice, and extending over a few lattice sites. The breathers have been found to persist indefinitely, and are either stationary or hopping in the lattice, depending on the precise make-up of the unit cell. We have observed that interacting breathers seem to repel each other when placed in close proximity which has the effect of (roughly) maintaining their pairwise distance in small periodic lattices.

This work paves the way for numerous studies. These include the detailed characterization of breathers, their stability and mobility properties and associated potential barrier in long (and infinite) 2D chains; the characterization of impurities and their role in inducing mobility; the examination of spectral gap and higher gap (nonlinear) states, especially in honeycomb lattices; and the generalization of such chains even in fully 3D configurations. These issues of broader interest to other settings such as Josephson-junction ladders [13] and granular crystals [14] will be considered in future publications.

[1] M.J. Ablowitz and D.E. Baldwin, Phys Rev. E **86**, 036305 (2012).
[2] K. Staliunas *et al.*, Phys. Rev. A **75**, 011604 (2007).
[3] S. Flach and A.V. Gorbach, Phys. Rep. **467**, 1 (2008).
[4] P.G. Kevrekidis, *The Discrete Nonlinear Schrödinger Equation*, Springer-Verlag (Heidelberg, 2009).
[5] F. Lederer *et al.*, Phys. Rep. **463**, 1 (2008).
[6] O. Morsch and M. Oberthaler, Rev. Mod. Phys. **78**, 179 (2006).
[7] M. Sato *et al.*, Rev. Mod. Phys. **78**, 137 (2006)
[8] P. Binder *et al.*, Phys. Rev. Lett. **84**, 745 (2000);

E. Trías *et al.*, Phys. Rev. Lett. **84**, 741 (2000).

[9] N. Boechler *et al.*, Phys. Rev. Lett. **104**, 244302 (2010).

[10] L.Q. English *et al.*, Phys. Rev. B **67**, 024403 (2003); U.T. Schwarz *et al.*, Phys. Rev. Lett. **83**, 223 (1999).

[11] B.I. Swanson *et al.*, Rev. Lett. **82**, 3288 (1999).

[12] M. Peyrard, Nonlinearity **17**, R1 (2004).

[13] J.J. Mazo Phys. Rev. Lett. **89**, 234101 (2002).

[14] A. Leonard and C. Daraio Phys. Rev. Lett. **108**, 214301 (2012).

[15] M.J. Ablowitz *et al.*, Phys. Rev. A **79**, 053830 (2009).

[16] O. Bahat-Treidel *et al.*, Phys. Rev. A **82**, 013830 (2010).

[17] C.L. Fefferman and M.I. Weinstein, arXiv:1202.3839.

[18] A.V. Savin and Yu.S. Kivshar, Phys. Rev. B **81**, 165418 (2010)

[19] M.I. Molina and Yu.S. Kivshar, Opt. Lett. **35**, 2895 (2010).

[20] L.Q. English et al., Phys. Rev. E **81**, 046605 (2010).

[21] F. Palmero *et al.*, Phys. Rev. E **84**, 026605 (2011).

[22] L.Q. English *et al.*, Phys. Rev. Lett. **108**, 084101 (2012).

[23] J.L Marín, J.C Eilbeck, and F.M Russell. Phys. Lett. A, **248**, 225 (1998).

[24] J.F.R. Archilla *et al.* J. Phys. Chem. **110**, 24112 (2006).